

Research Article

Evaluation of the Antihyperuricemic Activity of Phytochemicals from *Davallia formosana* by Enzyme Assay and Hyperuricemic Mice Model

Chen-Yu Chen,^{1,2} Chi-Chang Huang,³ Keng-Chang Tsai,⁴ Wei-Jan Huang,^{1,2}
Wen-Ching Huang,⁵ Yu-Chen Hsu,^{1,2} and Feng-Lin Hsu^{1,2}

¹ School of Pharmacy, College of Pharmacy, Taipei Medical University, Taipei 110, Taiwan

² Graduate Institute of Pharmacognosy, Taipei Medical University, Taipei 110, Taiwan

³ Graduate Institute of Sports Science, National Taiwan Sport University, Taoyuan 333, Taiwan

⁴ National Research Institute of Chinese Medicine, Taipei 112, Taiwan

⁵ Graduate Institute of Athletics and Coaching Science, National Taiwan Sport University, Taoyuan 333, Taiwan

Correspondence should be addressed to Feng-Lin Hsu; hsu0320@tmu.edu.tw

Received 22 December 2013; Revised 10 March 2014; Accepted 13 March 2014; Published 4 May 2014

Academic Editor: Wen Chuan Lin

Copyright © 2014 Chen-Yu Chen et al. This is an open access article distributed under the Creative Commons Attribution License, which permits unrestricted use, distribution, and reproduction in any medium, provided the original work is properly cited.

Abnormal serum urate levels are recognized as a critical factor in the progression of several chronic diseases. To evaluate the antihyperuricemic effect of *Davallia formosana*, the inhibitory activities of 15 isolated phytochemicals, including five novel compounds of 6,8-dihydroxychromone-7-*C*- β -*D*-glucopyranoside (1), 6,8,3',4'-tetrahydroxyflavanone-7-*C*- β -*D*-glucopyranoside (2), 6,8,4'-trihydroxyflavanone-7-*C*- β -*D*-glucopyranoside (3), 8-(2-pyrrolidinone-5-yl)-catechin-3-*O*- β -*D*-allopyranoside (4), and epiphylloumarin-3-*O*- β -*D*-allopyranoside (5), were examined against xanthine oxidase (XOD) and in a potassium oxonate-(PTO-) induced acute hyperuricemic mice model. The results indicated that compounds 3 and 5 significantly inhibited XOD activity *in vitro* and reduced serum uric acid levels *in vivo*. This is the first report providing new insights into the antihyperuricemic activities of flavonoid glycosides which can possibly be developed into potential hypouricemic agents.

1. Introduction

Hyperuricemia means high levels of uric acid in the blood, a condition considered to be closely associated with increased risks for developing gout, cardiovascular diseases, hypertension, and metabolic syndrome [1, 2]. Xanthine oxidase (XOD) is an important enzyme responsible for the catabolism of purines in humans; it oxidizes hypoxanthine into xanthine and then further forms uric acid [3, 4]. Allopurinol is currently the most effective XOD inhibitor, which is used for treating hyperuricemia and gout by reducing circulating levels of uric acid and vascular oxidative stress [5]. However, serious side effects include skin rashes and allergic reactions that occur in some clinical patients [6, 7].

Recently, several naturally occurring compounds were reported to inhibit XOD activity [8–10]. In particular, plant

phenolic compounds, such as phenolic acids and flavonoids, exhibit strong antioxidant activities via scavenging free radicals. Moreover, many studies also indicated that both types of compounds obviously inhibited XOD activity [11–13]. *Davallia formosana* is a popular herbal medicine used to treat osteoporosis [14]. Several flavan-3-ols, triterpenoids, proanthocyanidins, and mericprocyanidins were isolated from the rhizome of *D. formosana* [15, 16]. Our preliminary studies revealed that the crude extract of *D. formosana* rhizomes could inhibit XOD activity. Therefore, in this study, we investigated the constituents of *D. formosana* and their antihyperuricemic effects. An *in vitro* XOD-inhibitory assay and *in vivo* potassium oxonate- (PTO-) induced acute hyperuricemic mouse model were used to evaluate the uric acid-lowering effects of compounds isolated from *D. formosana*.

2. Materials and Methods

2.1. Chemicals and Reagents. PTO, allopurinol, sodium pyrophosphate, xanthine, and XOD were purchased from Sigma Chemical (St. Louis, MO). The solvents used for column chromatography, including methanol, *i*-BuOH, *n*-BuOH, dichloromethane (CH₂Cl₂), chloroform (CHCl₃), *n*-hexane, ethyl acetate (EtOAc), and acetone, were purchased from Merck (Darmstadt, Germany).

2.2. General Experimental Procedures. ¹H- and ¹³C-NMR spectra were obtained in the Bruker AM-500 spectrometer using corresponding solvents as internal standards. The optical rotation was measured on a Jasco DIP-1020 digital polarimeter. Electrospray ionization mass was determined on a VG platform electrospray mass spectrometer. Column chromatography was performed using Sephadex LH-20 (20~100 μm, Pharmacia Fine Chemicals, China), MCI-gel CHP 20P (75~150 μm, Mitsubishi Chemical Industries, Japan), Cosmosil C₁₈-OPN (75 μm, Nacalai Tesque), and silica gel 60 (70~230 mesh, Merck). Thin layer chromatography (TLC) was conducted on silica gel plates (60 F-254, Merck), with a 10% sulfuric acid solution as the visualizing agent on heating.

2.3. Plant Material. *Davallia formosana* was collected in Kaohsiung, Taiwan, in July 2010. It was authenticated by Dr. Hsien-Chang Chang (Division of Pharmacognosy, National Laboratories of Food and Drugs, Department of Health, Taiwan). A voucher specimen was deposited at the Department of Medicinal Chemistry, College of Pharmacy, Taipei Medical University, Taipei, Taiwan.

2.4. Extraction, Isolation, and Identification. Dry rhizomes of *D. formosana* (50 kg) were extracted with 80% ethanol at room temperature. The total ethanolic extract was evaporated in a vacuum. The residue (11 kg) was successively partitioned with *n*-hexane, EtOAc, and *n*-BuOH. The *n*-BuOH fraction (1.4 kg) was chromatographed on a Diaion HP20 column (25 × 120 cm) with a step gradient system (H₂O to MeOH, 1:0~0:1,50 L) to yield two fractions. The major fraction, DF-B (390 g), was further subjected to a Sephadex LH-20 column eluted with H₂O/MeOH (1:0~0:1) to afford four subfractions (DFB-1~4). The DFB-4 subfraction (263.7 g) was chromatographed over an MCI CHP20 (H₂O/MeOH 1:0~0:1) to obtain four subfractions (DFB-41~44). The DFB-43 subfraction (40.5 g) was subsequently purified on a Sephadex LH 20 (acetone) and silica gel with a CHCl₃-MeOH gradient to give **2** (62.0 mg), **3** (33.0 mg), **5** (115.0 mg), (-)-epicatech-3-*O*-β-D-(2''-*O*-vanillyl)-alloypyranoside (**7**, 760.0 mg), and (-)-epicatech-3-*O*-β-D-(3''-*O*-vanillyl)-alloypyranoside (**8**, 230.0 mg). (-)-Epicatech-3-*O*-β-D-alloypyranoside (**6**, 30.0 mg) was obtained by recrystallization (in acetone) of DFB-41 (37.3 g). The DFB-3 subfraction (30.3 g) was subjected to MCI CHP20 (H₂O to MeOH, 1:0~0:1) and Sephadex LH-20 (H₂O) column chromatography to yield **4** (5.0 mg), eriodictyol-8-*C*-β-D-glucopyranoside (**9**, 1.1 g), davallioside A (**10**, 31.0 mg), davallioside B (**11**, 20.0 mg), and caffeic

acid-4-*O*-β-D-glucopyranoside (**12**, 210.0 mg). The DFB-2 fraction (62.4 g) was subjected to MCI CHP20 column chromatography with H₂O/MeOH gradient system to give eight subfractions (DFB-21~28). Subfraction DFB-23 (17.7 g) from H₂O eluent was purified by MCI CHP20 gel and Sephadex LH-20 column to yield **1** (537.0 mg) and *p*-coumaric acid-4-*O*-β-D-glucopyranoside (**13**, 92.7 mg).

Protocatechuic acid (**14**, 730.0 mg), 4-hydroxy-3,5-dimethylbenzoic acid (**15**, 97.3 mg), vanillic acid (**16**, 86.0 mg), 4-hydroxy-3-aminobenzoic acid (**17**, 60.0 mg), and (-)-epicatechin (**18**, 202.0 mg) were obtained from EtOAc fraction (170.0 g). Davallic acid (**19**, 6.0 g) and β-stiosterol (**20**, 644.0 mg) were isolated from *n*-hexane fraction (114.0 g).

6,8-Dihydroxychromone-7-*C*-β-D-glucopyranoside (1). White amorphous powder; [α]_D²⁴ - 91.2° (*c* = 0.5, MeOH); IR (KBr) ν_{max}: 3332, 1650, 1631, 1568 cm⁻¹; UV (MeOH) λ_{max}: 210, 258, and 298 nm; HR-ESI-MS *m/z*: 339.0717 [M-H]⁻ (calcd. for C₁₅H₁₅O₉, 339.0716).

6,8,3',4'-Tetrahydroxyflavanone-7-*C*-β-D-glucopyranoside (2). White amorphous powder; [α]_D²⁴ - 43.2° (*c* = 1.0, MeOH); IR (KBr) ν_{max}: 3250, 1652, 1584, 1539 cm⁻¹; UV (MeOH) λ_{max}: 205.0 and 288.5 nm; HR-ESI-MS *m/z*: 449.1087 [M-H]⁻ (calcd. for C₂₁H₂₁O₁₁, 449.1084).

6,8,4'-Trihydroxyflavanone-7-*C*-β-D-glucopyranoside (3). White amorphous powder; [α]_D²⁴ - 21.8° (*c* = 0.5, MeOH); IR (KBr) ν_{max}: 3315, 1615, 1518 cm⁻¹; UV (MeOH) λ_{max}: 226.0 and 290.0 nm; HR-ESI-MS *m/z*: 433.1142 [M-H]⁻ (calcd. for C₂₁H₂₁O₁₀, 433.1135).

8-(2-Pyrrolidinone-5-yl)-catechin-3-*O*-β-D-alloypyranoside (4). Yellow amorphous solid; [α]_D²⁴ + 9.7° (*c* = 1.0, MeOH); IR (KBr) ν_{max}: 3334, 1646, 1611 cm⁻¹; UV (MeOH) λ_{max}: 209 and 280 nm; HR-ESI-MS *m/z*: 534.1617 [M-H]⁻ (calcd. for C₂₅H₂₈NO₁₂, 534.1612).

Epiphyllocoumarin-3-*O*-β-D-alloypyranoside (5). White amorphous powder; [α]_D²⁴ - 96.7° (*c* = 0.2, MeOH); IR (KBr) ν_{max}: 3314, 1707, 1613, 1573, 1531 cm⁻¹; UV (MeOH) λ_{max}: 208 and 334 nm; HR-ESI-MS *m/z*: 503.1203 [M-H]⁻ (calcd. for C₂₄H₂₃O₁₂, 503.1190).

Acid hydrolysis of 5. Compound **5** (10 mg) was hydrolyzed with 2 N HCl in aqueous MeOH (5 mL) for 4 h, and the product was further extracted with EtOAc. The H₂O layer was passed through silica gel eluted with CHCl₃/MeOH/H₂O (4:2:0.1) to give a sugar residue. The sugar was analyzed by silica gel TLC [*i*-PrOH-Me₂CO-H₂O (5:3:1), R_f 0.55] and compared to authentic samples.

2.5. Determination of XOD-Inhibitory Activity. The inhibitory effect on XOD was determined spectrophotometrically [17]. The reaction mixture consisted of 100 μL of 50 mM potassium phosphate buffer (pH 7.5), 50 μL of 1.5 mM

xanthine, 10 μL of sample solution dissolved in dimethyl sulfoxide (DMSO), and 25 μL XOD (0.05 U). The absorption increments at a UV absorbance of 295 nm indicated the formation of uric acid. All determinations were performed in triplicate. Pure compounds and allopurinol for the XO inhibitory activity assays were examined at concentrations of 0, 25, 50, and 100 μM , respectively. The inhibitory activity of XOD was assessed as the inhibitory percent (%) = $(1 - b/a) \times 100$, where “a” is the change in absorbance per minute without the sample, and “b” is the change in absorbance per minute with the sample.

2.6. Hypouricemic Effects Examined in Mice with PTO-Induced Hyperuricemia. Six-week-old male ICR mice with body weights of about 30.0 g were purchased from BioLASCO (A Charles River Licensee Corp., Yilan, Taiwan). Before the experiments, mice were raised for 1 week to allow them to acclimate to the environment and diet. All mice were given a standard laboratory diet (no. 5001; PMI Nutrition International, Brentwood, MO) and distilled water *ad libitum* and kept on a 12 h light/dark cycle at $22 \pm 2^\circ\text{C}$. This study was conducted according to institutional guidelines and was approved by the Institutional Animal Care and Utilization Committee (IACUC) of National Taiwan Sport University, Taoyuan, Taiwan. This study was approved by the IACUC ethics committee under protocol IACUC-10004.

Test animals were intraperitoneally (*i.p.*) injected with phosphate-buffered saline (PBS) containing 200 mg/kg of PTO 1 h before administration of test samples adapted from recent studies [18, 19]. Mice were randomly divided into six groups for treatment ($n = 6$): (1) a vehicle group; (2) PTO group; (3) PTO + allopurinol (AP) group; (4) PTO + 2 group; (5) PTO + 3 group; (6) PTO + 5 group. For the comparative study, the same dosages of 100 mmol/kg of AP (13.6 mg/kg), compound 2 (45.0 mg/kg), compound 3 (43.4 mg/kg), and compound 5 (50.4 mg/kg) were delivered *i.p.* at 1 h after PTO administration. Blood samples were centrifuged at $1400 \times g$ and 4°C for 15 min, and the level of serum uric acid was determined by a commercial kit from Randox Laboratories (UK).

2.7. Xanthine Oxidase Molecular Docking. Models of compound 5 in complex with xanthine oxidase were generated through docking compound 5 to the active site of the X-ray crystal structure of bovine xanthine oxidase (PDB id: 3B9J) (Figure 5). In order to predict the position of compound 5 in the active site, we implemented the docking program (GOLD Genetic Optimization for Ligand Docking) (Cambridge Crystallographic Data Center (CCDC), version 3.2) with the Goldscore scoring function. Before docking, the substrate 2-hydroxy-6-methylpurine and all water molecules were removed. The 3D structure of compound 5 was generated and optimized by energy minimization using Discovery Studio v.3.5 (Accelrys Software Inc., USA). GOLD was used to dock compound 5 into the proteins with the flexible docking option turned on. Initially, 500 independent genetic algorithm cycles of computation were carried out with ligand torsion angles varying between -180° and 180° . The search

efficiency was set at 200% to ensure the most exhaustive search for the docking conformational space. All other parameters were kept the same as the default settings. Finally, from the 500 docking conformations of compound 5, the top one with the highest GOLD fitness score was chosen to explore the “inhibitor-bond” conformations in the xanthine oxidase active site using Goldscore within the GOLD program. The molecular models of compound 5 were displayed using the PyMOL software (<http://www.pymol.org>).

2.8. Statistical Analysis. All data are expressed as the mean \pm standard error of the mean (SEM). A one-way analysis of variance (ANOVA) was performed with Duncan's post hoc test for multisample testing. $P < 0.05$ was considered statistically significant.

3. Results and Discussion

3.1. Structure Elucidation. The rhizome of *D. formosana* was extracted with 80% ethanol and repeatedly chromatographed to obtain 20 compounds. Five new compounds (Figure 1) together with 15 known compounds, including seven flavonoids, six phenolics, and two triterpenoids, were elucidated based on the physical and spectral data.

Compound 1 was obtained as a white amorphous powder. The HR-ESI-MS analysis agreed with the molecular formula $\text{C}_{15}\text{H}_{16}\text{O}_9$ ($m/z = 339.0717$ $[\text{M}-\text{H}]^-$). The ^1H and ^{13}C -NMR data showed typical signals of a flavone nucleus and a glucose unit. Resonances of the flavone moiety were assigned at δ 8.02 (1H, d, $J = 6.1$ Hz, H-2), 6.27 (1H, d, $J = 6.1$ Hz, H-3), and δ 6.50 (1H, s, H-5). The deshielding of the chemical shifts at δ 163.3 and 160.5 indicated a 6,8-dihydroxyl substitution. Glucose signals were determined by ^1H - ^1H COSY and HMQC spectra. The site of the glucose linkage to the flavone was considered to be C-7 from the HMBC experiment. These results suggested that the structure of compound 1 was 6,8-dihydroxychromone-7-C- β -D-glucopyranoside.

Compound 2 was isolated as a white amorphous powder with optical rotation $[\alpha]_D^{24} - 43.2^\circ$. The negative HR-ESI-MS exhibited quasimolecular ion peaks at m/z 449.1087 $[\text{M}-\text{H}]^-$. ^1H -NMR and ^1H - ^1H COSY spectra showed typical flavanone structural features at δ 5.91 (1H, s, H-5), 5.34 (1H, dd, $J = 11.9, 2.8$ Hz, H-2), 2.70 (1H, dd, $J = 17.9, 3.1$ Hz, H-3), and 3.03–3.16 (1H, m, H-3). The coupling constant of 17.9 Hz observed at δ 2.70 indicated that the C-2 substituted aryl group was equatorial. The ABX-type resonance at δ 6.85 (1H, s, H-2'), 6.74 (1H, d, $J = 8.5$ Hz, H-6'), and 6.68 (1H, d, $J = 8.5$ Hz, H-5') indicated the presence of 1,3,4-trisubstitutions in the B-ring. Additionally, the ^1H -NMR spectrum exhibited signals at δ 3.03–4.46 for a sugar moiety. The COSY and HMQC spectra indicated that the sugar moiety was a glucopyranose. The β -configuration of the glucose moiety was determined by the coupling constant of an anomeric proton ($J = 9.8$ Hz). The resonances of C-6 and C-8 were significantly shifted downfield to δ 166.3 and 162.0, and the HMBC spectrum showed a correlation between the aromatic proton (δ 5.91) and carbonyl carbon (δ 196.9). This evidence indicated that hydroxyl groups were substituted at

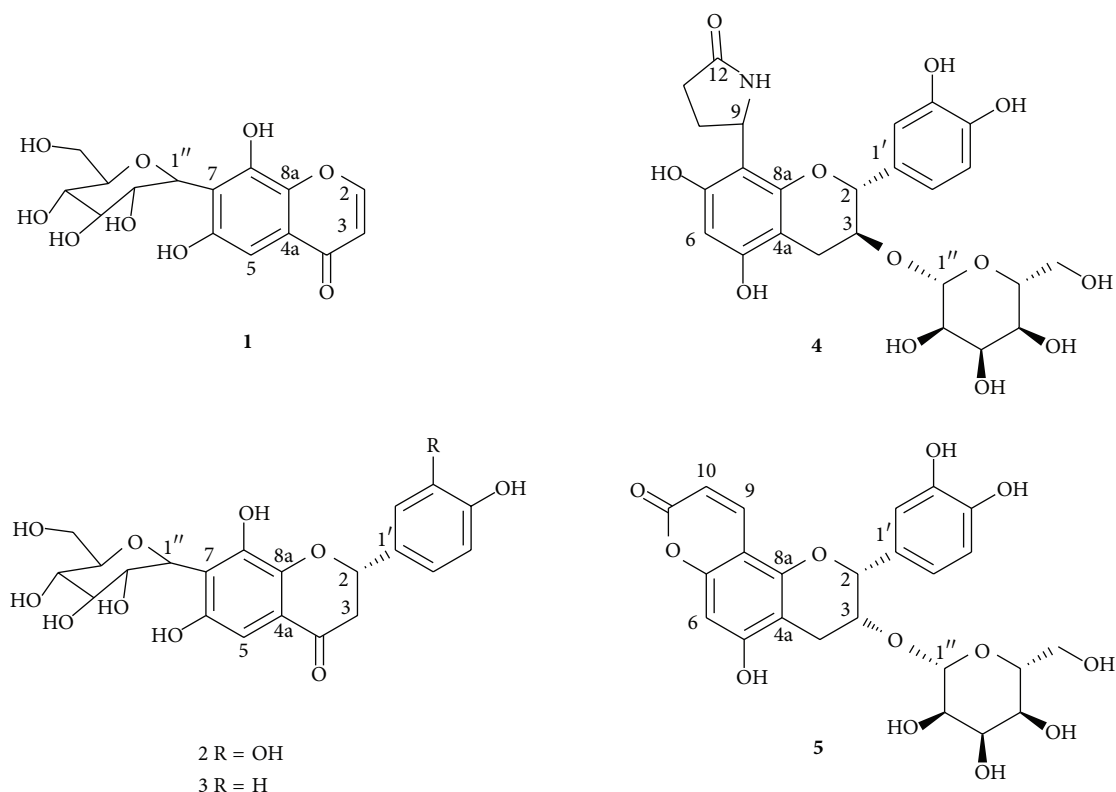


FIGURE 1: Chemical structures of new compounds 1-5 isolated from the rhizome of *Davallia formosana*.

C-6, 8. Moreover, the HMBC experiment further showed the three-bond correlation between the anomeric proton H-1'' (δ 4.46) and C-6, 8 (δ 166.3, 162.0), suggesting that the glucose was joined to the A-ring of the aglycone through a C-glycosidic linkage at C-7. Therefore, the structure of 2 was characterized as 6,8,3',4'-tetrahydroxyflavanone-7-C- β -D-glucopyranoside.

The molecular formula of compound 3 was established as C₂₁H₂₂O₁₀ on the basis of HR-ESI-MS data (m/z 433.1142 for [M-H]⁻). The ¹H-NMR spectrum of 3 was similar to that of 2, except that the AX-type resonance at δ 6.81 and 7.31 (each 2H, J = 8.5 Hz) replaced the ABX-type coupling pattern of compound 2. Six carbon signals at δ 82.9, 80.8, 75.5, 72.9, 72.2, and 63.2 were assigned as a glucopyranose. The orientation of glucose was confirmed to be the β -configuration according to the coupling constant of the anomeric proton (J = 9.8 Hz). The HMBC correlation between glucopyranose H-1'' and aglycone C-7 suggested that glucose was substituted at C-7 of the aglycone. The molecular weight of 3 lost 16 units compared to that of 2, which supported compound 3 having lost a hydroxyl group at position C-5'. Accordingly, the structure of compound 3 was assigned as 6,8,4'-trihydroxyflavanone-7-C- β -D-glucopyranoside.

Compound 4 was isolated as a yellow amorphous solid. The molecular formula was deduced to be C₂₅H₂₉NO₁₂ from HR-ESI-MS at m/z 534.1628 [M-H]⁻. According to the ¹H and ¹³C-NMR data, the compound showed a characteristic catechin structure feature at δ 5.07 (1H, d, J = 5.5 Hz,

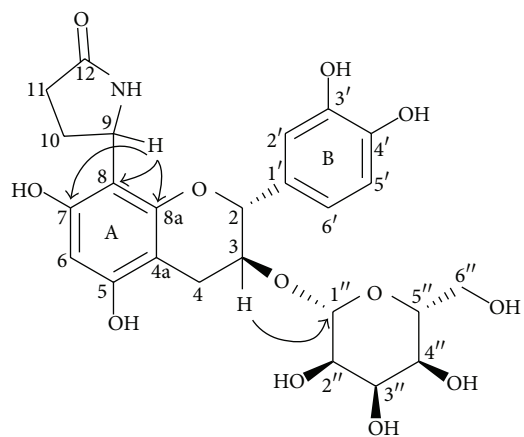


FIGURE 2: HMBC correlations of compound 4.

H-2), 4.32 (1H, m, H-3), and 2.70 (2H, d, J = 5.5 Hz, H-4). The $J_{2,3}$ coupling constant (J = 5.5 Hz) confirmed the *trans*-arrangement of H-2 and H-3. Analysis of ¹H-¹H COSY and HMQC spectra, the deshielding of the carbonyl signal at δ 181.6, a tertiary carbon signal at δ 50.3 (C-11), and two methylene signals at δ 32.3, 27.0 indicated that a γ -lactam group was contained in the structure. This result was further demonstrated by IR absorption at 1646 cm⁻¹. The long-range correlation between the signal at δ 5.37 (1H, dd, J = 9.5, 4.6 Hz, H-11) and C-7, 8, 8a suggested that the γ -lactam ring was attached to C-8 (Figure 2). The allopyranose

moiety was determined by ^1H - ^1H COSY and HMBC spectra. Additionally, the HMBC correlation between H-3 and C-1'' demonstrated that the allopyranose residue was linked to C-3 of the aglycone. These results indicated that compound 4 was similar to davallioside A and B [20]. Therefore, compound 4 was a catechin-3-*O*- β -D-allopyranoside with a γ -lactam substitution at C-8, and it was determined by 8-(2-pyrrolidinone-5-yl)-catechin-3-*O*- β -D-allopyranoside.

Compound 5 was a white amorphous powder, and the molecular formula was determined to be $\text{C}_{24}\text{H}_{24}\text{O}_{12}$ (m/z 503.1203 for $[\text{M}-\text{H}]^-$) by the HR-ESI-MS spectrum. The ^1H and ^{13}C -NMR data (Supplementary Tables 1 and 2 available online at <http://dx.doi.org/10.1155/2014/873607>) showed that compound 5 was comprised of three units, including a flavan-3-ol, a sugar unit, and an α,β -unsaturated carbonyl group. The relative configurations at H-2 and H-3 were assigned as a *cis*-orientation based on the coupling constant of signals at δ 5.32 (1H, br.s, H-2) and 4.44 (1H, d, $J = 2.4$ Hz, H-3). The methylene protons at δ 2.81 (1H, dd, $J = 16.2, 4.3$ Hz) and 2.65 (1H, dd, $J = 16.2, 5.2$ Hz) of H-4 indicated a flavan moiety structure of compound 5. Resonances of four aromatic protons included a typical ABX-type spin system of the 1,3,4-trisubstituted benzene ring [δ 6.95 (br.s, H-2'), 6.76 (d, $J = 8.5$ Hz, H-5'), and 6.66 (d, $J = 8.5$ Hz, H-6')] and one singlet at δ 6.38 attributed to the A-ring of flavan-3-ol. The HMBC correlations between the olefinic proton δ 7.99 (H-10) and C-8 (δ 101.8), as well as δ 6.10 (H-9) and C-7 (δ 154.7), indicated an α,β -unsaturated carbonyl group linked to the C-7, 8 of A-ring. These results revealed that these resonances were consistent with the pyrone ring of a coumarin entity [21]. Acid hydrolysis of 5 yielded epiphylloucoumarin [22] and allopyranose. The β -configuration of the sugar moiety was determined by the coupling constant of the anomeric proton δ 4.51 (1H, d, $J = 7.3$ Hz, H-1'). The HMBC correlation of H-3 to C-1' demonstrated that the allopyranose residue was linked to C-3 of the aglycone. Therefore, 5 was characterized as epiphylloucoumarin-3-*O*- β -D-allopyranoside.

Fifteen known compounds, including (-)-epicatech-3-*O*- β -D-allopyranoside (6) [23], (-)-epicatech-3-*O*- β -D-(2''-*O*-vanillyl)-allopyranoside (7) [16], (-)-epicatech-3-*O*- β -D-(3''-*O*-vanillyl)-allopyranoside (8) [16], eriodictyol-8-*C*- β -D-glucopyranoside (9) [24], davallioside A (10) [20], davallioside B (11) [20], caffeic acid-4-*O*- β -D-glucopyranoside (12) [25], *p*-coumaric acid-4-*O*- β -D-glucopyranoside (13) [25], protocatechuic acid (14) [26], 4-hydroxy-3,5-dimethylbenzoic acid (15) [27], vanillic acid (16) [28], 4-hydroxy-3-aminobenzoic acid (17) [29], (-)-epicatechin (18) [30], davallialic acid (19) [15], and β -sitosterol (20) [31], were identified by comparison with values in the literature. Among them, compounds 9-17 were first isolated from *D. formosana*.

3.2. The XOD-Inhibitory Activity of Phytochemicals from *D. formosana*. The XOD-inhibitory activities of all pure compounds isolated from *D. formosana* were examined with effects comparable to that of allopurinol (Supplementary Table 3), a clinically used inhibitor, at the same concentration. Compounds 3 and 5 significantly inhibited XOD

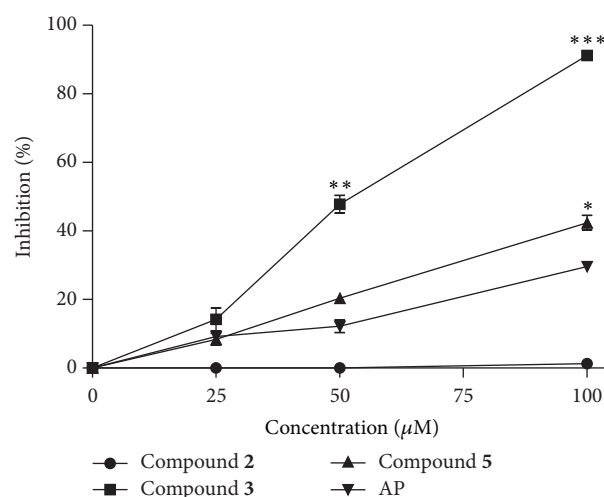


FIGURE 3: The xanthine oxidase- (XOD-) inhibitory activity of phytochemicals from *Davallia formosana*. AP, allopurinol (positive control); 2, 6,8,3',4'-tetrahydroxyflavanone-7-*C*- β -D-glucopyranoside; 3, 6,8,4'-trihydroxyflavanone-7-*C*- β -D-glucopyranoside; 5, epiphylloucoumarin-3-*O*- β -D-allopyranoside. Each value represents the mean \pm SEM of three replicates. * $P < 0.05$, ** $P < 0.01$, and *** $P < 0.001$, compared to the positive control.

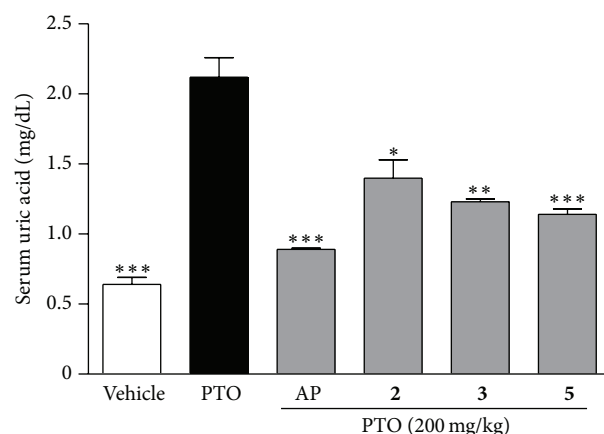


FIGURE 4: The uric acid-lowering effects of compounds 2, 3, and 5 from *Davallia formosana* on mice with potassium oxonate- (PTO-) induced hyperuricemia. The results are presented as the mean \pm SEM ($n = 6$). * $P < 0.005$, ** $P < 0.001$, and *** $P < 0.0001$, compared to the PTO-treated group.

activity in dose-dependent manners, compared to allopurinol (Figure 3). The IC_{50} of compounds 3 and 5 was 57.4 and 124.0 μM , respectively, whereas there was no detectable effect for compound 2.

3.3. In Vivo Hypouricemic Effect Determined in Mice with PTO-Induced Hyperuricemia. To further confirm the capabilities of compounds 2, 3, and 5 to reduce the uric acid level *in vivo*, a PTO-induced hyperuricemia mice model was investigated. After 3 h of PTO treatment, the level of serum uric acid had increased to 12 ± 0.14 mg/dL. As shown in Figure 4, PTO-induced serum uric acid levels were reduced by

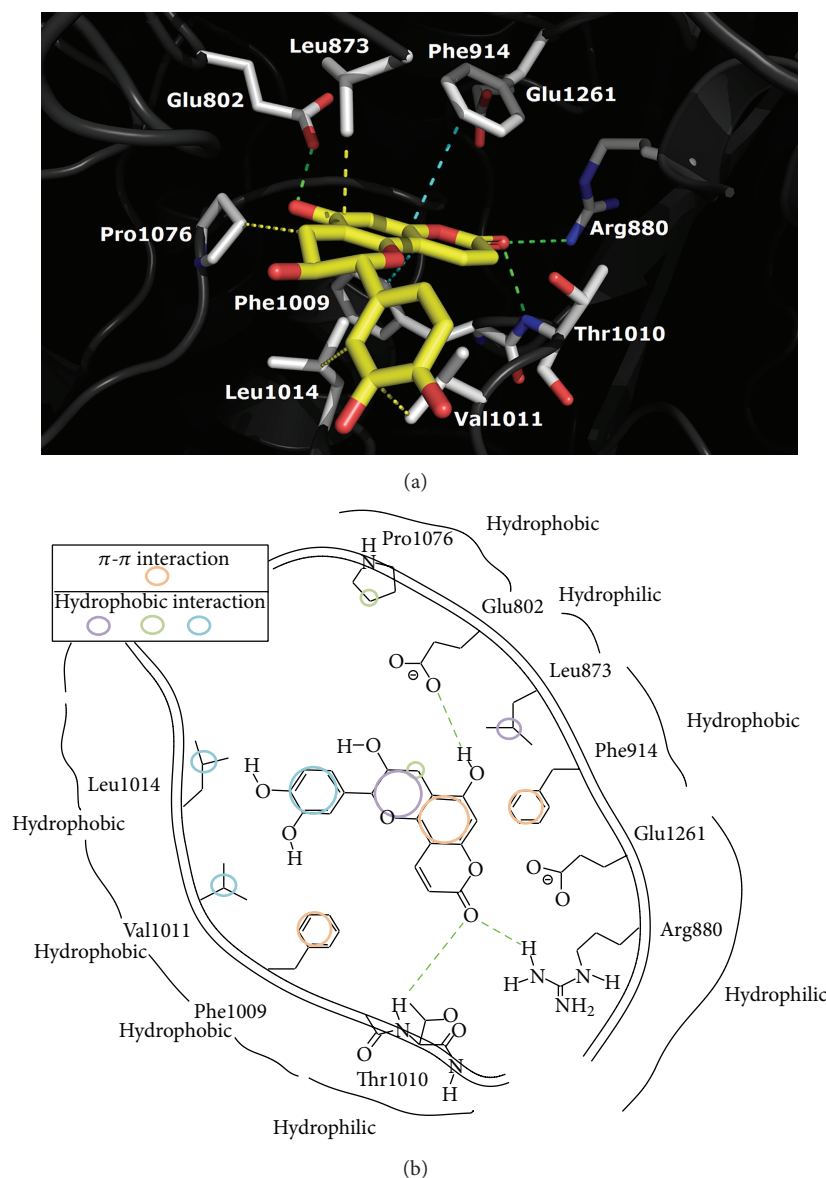


FIGURE 5: Predicted binding mode of compound 5 docked into the active site of xanthine oxidase. The top and down pictures of each panel display the 3D and 2D structural docking patterns, respectively. The nitrogen and oxygen atoms are shown in dark blue and red colors, respectively. The hydrogen bond formation and the electrostatic interaction between compound 5 (yellow) and the amino acid residues (gray) of XOD are shown in green and light blue dashed lines, respectively.

the three test compounds, as well as the reference (allopurinol). At the same concentration (100 mmol/kg), compounds 2, 3, 5, and allopurinol significantly reduced the level of serum uric acid by 33.9%, 41.7%, 46.0%, and 58.1%, respectively, compared to the PTO group ($P < 0.005$). XOD is an important purine metabolic enzyme, which is a significant target for developing antihyperuricemic drugs. The *in vitro* and *in vivo* results suggested that inhibition of XOD activity played an important role in the antihyperuricemic effects of compounds 3 and 5.

3.4. Computational Docking Studies of Compound 5. In addition to its uric acid-lowering activity *in vivo*, compound 5 also inhibits xanthine oxidase activity *in vitro*. We were

interested in visualizing the effects of compound 5 on XOD in order to gain insights into the observed activities. Many studies have shown that flavonoids can inhibit XOD activity via hydrogen bonding and hydrophobic interaction with key amino acid residues on XOD-catalyzed sites such as Arg880, Phe914, Phe1009, and Thr1010 [32]. To determine the preferred positions of binding sites on XOD for compound 5, the 3D model of interaction was analyzed by docking using bovine milk XOD (PDB id: 3B9J)[33].

As shown in Figure 5, the carbonyl group on the benzopyranone forms hydrogen bonds with the active sites, including Arg880 and Thr1010. Furthermore, the 5-hydroxyl group of compound 5 forms hydrogen bonds with Glu802. The docking results show again that the A-ring of compound

5 is sandwiched between Phe914 and Phe1009 and participates in the formation of aromatic interactions ($\pi - \pi$ effects) with the two phenylalanines. In addition, three hydrophobic interactions were observed involving the methylene and Pro1076, the 3',4'-dihydroxyphenyl moiety and Leu1014, and Val1011. It can be seen that binding residues are the same among [34], suggesting that Arg880 and Thr1010 might be of significance for the selective inhibition of XOD by compound 5.

This study obtained five new compounds from *D. formosana*, and two of them exhibited potent antihyperuricemic activity. Accordingly, our results can provide the scientific basis for development of antihyperuricemic drugs.

Conflict of Interests

All authors declare that they have no conflict of interests.

Authors' Contribution

Chi-Chang Huang and Keng-Chang Tsai contributed equally to this work.

Acknowledgments

The authors thank Dr. Hsien-Chang Chang for helping identify the plant material. They are grateful to Ms. Shu-Yun Sun (Taipei Regional Analytical Instrumentation Center, NSC) for measurement of the high-resolution ESIMS and Ms. Shwu-Hui Wang (Center for Instrumentation, Taipei Medical University) for measurement of the NMR spectra. They are grateful to the National Center for High-Performance Computing for allowing them to use their computer facilities. This study was supported by a Grant from the National Science Council of Taiwan (NSC101-2320-B-038-012-MY2).

References

- [1] M. A. Becker and M. Jolly, "Hyperuricemia and associated diseases," *Rheumatic Disease Clinics of North America*, vol. 32, no. 2, pp. 275–293, 2006.
- [2] R. L. Wortmann, "Gout and hyperuricemia," *Current Opinion in Rheumatology*, vol. 14, no. 3, pp. 281–286, 2002.
- [3] A. Agarwal, A. Banerjee, and U. C. Banerjee, "Xanthine oxidoreductase: a journey from purine metabolism to cardiovascular excitation-contraction coupling," *Critical Reviews in Biotechnology*, vol. 31, no. 3, pp. 264–280, 2011.
- [4] R. Harrison, "Structure and function of xanthine oxidoreductase: where are we now?" *Free Radical Biology and Medicine*, vol. 33, no. 6, pp. 774–797, 2002.
- [5] G. B. Elion, "The purine path to chemotherapy," *Science*, vol. 244, no. 4900, pp. 41–47, 1989.
- [6] R. Shalom, S. Rimbroth, D. Rozenman, and A. Markel, "Allopurinol-induced recurrent DRESS syndrome: pathophysiology and treatment," *Renal Failure*, vol. 30, no. 3, pp. 327–329, 2008.
- [7] T. Gibson, "Hyperuricemia, gout and the kidney," *Current Opinion in Rheumatology*, vol. 24, no. 2, pp. 127–131, 2012.
- [8] G. Sahgal, S. Ramanathan, S. Sasidharan, M. N. Mordi, S. Ismail, and S. M. Mansor, "In Vitro antioxidant and xanthine oxidase inhibitory activities of methanolic *Swietenia mahagoni* seed extracts," *Molecules*, vol. 14, no. 11, pp. 4476–4485, 2009.
- [9] H. Konno, Y. Kanai, M. Katagiri et al., "Melinjo (*Gnetum gnemon* L.) seed extract decreases serum uric acid levels in nonobese Japanese males: a randomized controlled study," *Evidence-Based Complementary and Alternative Medicine*, vol. 2013, Article ID 589169, 9 pages, 2013.
- [10] A. P. Sweeney, S. G. Wyllie, R. A. Shalliker, and J. L. Markham, "Xanthine oxidase inhibitory activity of selected Australian native plants," *Journal of Ethnopharmacology*, vol. 75, no. 2–3, pp. 273–277, 2001.
- [11] A. Crozier, I. B. Jaganath, and M. N. Clifford, "Dietary phenolics: chemistry, bioavailability and effects on health," *Natural Product Reports*, vol. 26, no. 8, pp. 1001–1043, 2009.
- [12] C. Spanou, A. S. Veskokoukis, T. Kerasioli et al., "Flavonoid glycosides isolated from unique legume plant extracts as novel inhibitors of xanthine oxidase," *PLoS ONE*, vol. 7, no. 3, Article ID e32214, 2012.
- [13] N. Wu, Y. Zu, Y. Fu et al., "Antioxidant activities and xanthine oxidase inhibitory effects of extracts and main polyphenolic compounds obtained from *geranium sibiricum* L.," *Journal of Agricultural and Food Chemistry*, vol. 58, no. 8, pp. 4737–4743, 2010.
- [14] Y. J. Ko, J. B. Wu, H. Y. Ho, and W. C. Lin, "Antiosteoporotic activity of *Davallia formosana*," *Journal of Ethnopharmacology*, vol. 139, no. 2, pp. 558–565, 2012.
- [15] Y. Y. Lin, H. Kakisawa, Y. Shiobara, and K. Nakanishi, "The structure of davallic acid," *Chemical and Pharmaceutical Bulletin*, vol. 13, no. 8, pp. 986–995, 1965.
- [16] T. H. Hwang, Y. Kashiwada, G. Nonaka, and I. Nishioka, "Flavan-3-ol and proanthocyanidin allosides from *Davallia divaricata*," *Phytochemistry*, vol. 28, no. 3, pp. 891–896, 1989.
- [17] Y. T. Tung and S. T. Chang, "Inhibition of xanthine oxidase by acacia confusa extracts and their phytochemicals," *Journal of Agricultural and Food Chemistry*, vol. 58, no. 2, pp. 781–786, 2010.
- [18] Y. T. Tung, C. A. Hsu, C. S. Chen, S. C. Yang, C. C. Huang, and S. T. Chang, "Phytochemicals from *Acacia confusa* heartwood extracts reduce serum uric acid levels in oxonate-induced mice: their potential use as xanthine oxidase inhibitors," *Journal of Agricultural and Food Chemistry*, vol. 58, no. 18, pp. 9936–9941, 2010.
- [19] S. T. Ho, Y. T. Tung, C. C. Huang et al., "The hypouricemic effect of *Balanophora laxiflora* extracts and derived phytochemicals in hyperuricemic mice," *Evidence-Based Complementary and Alternative Medicine*, vol. 2012, Article ID 910152, 7 pages, 2012.
- [20] C.-B. Cui, Y. Tezuka, T. Kikuchi, H. Nakano, and J.-H. Park, "Davallioside A and B, novel flavin-3-ol derivatives with a γ -lactam, from the rhizomes of *Davallia mariesii* Moore," *Chemical and Pharmaceutical Bulletin*, vol. 38, no. 9, pp. 2620–2622, 1990.
- [21] M. K. Bhan, S. Raj, M. N. S. Nayar, and K. L. Handa, "Isoprenylcoumarins from *Boenninghausenia albiflora*," *Phytochemistry*, vol. 12, no. 12, pp. 3010–3011, 1973.
- [22] L. Y. Foo, "Flavanocoumarins and flavanophenylpropanoids from *Phyllocladus trichomanoides*," *Phytochemistry*, vol. 28, no. 9, pp. 2477–2481, 1989.
- [23] C.-B. Cui, Y. Tezuka, T. Kikuchi, H. Nakano, T. Tamaoki, and J.-H. Park, "Constituents of a fern, *Davallia mariesii* Moore. IV.

- Isolation and structures of a novel norcarotane sesquiterpene glycoside, a chromone glucuronide, and two epicatechin glycosides," *Chemical and Pharmaceutical Bulletin*, vol. 40, no. 8, pp. 2035–2040, 1992.
- [24] F. L. Hsu and J. Y. Chen, "Phenolics from *Tectaria subtriphylla*," *Phytochemistry*, vol. 34, no. 6, pp. 1625–1627, 1993.
- [25] C.-B. Cui, Y. Tezuka, T. Kikuchi, H. Nakano, T. Tamaoki, and J.-H. Park, "Constituents of a fern, *Davallia mariesii* Moore. I. Isolation and structures of davallialactone and a new flavanone glucuronide," *Chemical and Pharmaceutical Bulletin*, vol. 38, no. 12, pp. 3218–3225, 1990.
- [26] K. N. Scott, "Carbon-13 nuclear magnetic resonance of biologically important aromatic acids. I. Chemical shifts of benzoic acid and derivatives," *Journal of the American Chemical Society*, vol. 94, no. 24, pp. 8564–8568, 1972.
- [27] Y. Lu, T. K. Lum, Y. W. L. Augustine et al., "Replacement of the N-terminal tyrosine residue in opioid peptides with 3-(2,6-dimethyl-4-carbamoylphenyl)propanoic acid (Dcp) results in novel opioid antagonists," *Journal of Medicinal Chemistry*, vol. 49, no. 17, pp. 5382–5385, 2006.
- [28] L. J. Harrison, S. G. Sia Guat-Lee, S. K. Sim Keng-Yeow et al., "A ferulic acid ester of sucrose and other constituents of *Bhesa paniculata*," *Phytochemistry*, vol. 38, no. 6, pp. 1497–1500, 1995.
- [29] D. Xu, A. Chiaroni, M. Fleury, and M. Largeton, "Electrochemically induced cascade reaction for the assembly of libraries of biologically relevant 1,4-benzoxazine derivatives," *Journal of Organic Chemistry*, vol. 71, no. 17, pp. 6374–6381, 2006.
- [30] A. L. Davis, Y. Cai, A. P. Davies, and J. R. Lewis, "¹H and ¹³C NMR assignments of some green tea polyphenols," *Magnetic Resonance in Chemistry*, vol. 34, no. 11, pp. 887–890, 1996.
- [31] S. Priyashree, S. Jha, and S. Pattanayak, "A review on *Cressa cretica* Linn.: a halophytic plant," *Pharmacognosy Reviews*, vol. 4, no. 8, pp. 161–166, 2010.
- [32] C.-M. Lin, C.-S. Chen, C.-T. Chen, Y.-C. Liang, and J. Lin, "Molecular modeling of flavonoids that inhibits xanthine oxidase," *Biochemical and Biophysical Research Communications*, vol. 294, no. 1, pp. 167–172, 2002.
- [33] J. M. Pauff, J. Zhang, C. E. Bell, and R. Hille, "Substrate orientation in xanthine oxidase: crystal structure of enzyme in reaction with 2-hydroxy-6-methylpurine," *Journal of Biological Chemistry*, vol. 283, no. 8, pp. 4818–4824, 2008.
- [34] J. Yan, G. Zhang, Y. Hu, and Y. Ma, "Effect of luteolin on xanthine oxidase: inhibition kinetics and interaction mechanism merging with docking simulation," *Food Chemistry*, vol. 141, no. 4, pp. 3766–3773, 2013.



Hindawi

Submit your manuscripts at
<http://www.hindawi.com>

